Analytical Methods

Microfluidic Platform for the Enzymatic Pretreatment of Human Serum for the Detection of the Tuberculosis Biomarker Mannose-Capped Lipoarabinomannan

Journal:	*Analytical Methods*
Manuscript ID	AY-TEC-04-2024-000772.R1
Article Type:	Technical Note
Date Submitted by the Author:	28-Jun-2024
Complete List of Authors:	Lambert, Christopher; University of Utah, Mechanical Engineering; University of Utah Mechanical Engineering Clarke, Eamonn; University of Utah, Chemical Engineering Patel, Dhruv; U of U, Mechanical Engineering Laurentius, Lars; University of Utah, Nano Institute of Utah Gale, Bruce; University of Utah, Mechanical Engineering Sant, Himanshu; University of Utah, Chemical Engineering Porter, Marc; University of Utah, Chemistry

Microfluidic Platform for the Enzymatic Pretreatment of Human Serum for the Detection of the Tuberculosis Biomarker Mannose-Capped Lipoarabinomannan

Christopher J. Lambert[1]*, Eamonn Clarke[2†], Dhruv Patel[1†], Lars B. Laurentius[3], Bruce K. Gale[1], Himanshu J. Sant[1†], Marc D. Porter[2,4‡]
Departments of Mechanical Engineering[1], Chemistry[2], Electrical and Computer Engineering[3] and Chemical Engineering[4], University of Utah, Salt Lake City, UT, USA 84112
*Present address: Colossal Biosciences, Austin, TX, USA 78701
†Present address: Department of Chemical Engineering, University of Utah, Salt Lake City, UT, USA 84112
‡Author to whom correspondence should be addressed

Abstract

Tuberculosis (TB) represents a major public health threat, with millions of new cases reported worldwide each year. A major hurdle to curtailing the spread of this disease is the need for low-cost, point-of-care (PoC) diagnostics. Mannose-capped lipoarabinomannan, a significant component of the *Mycobacterium tuberculosis* bacillus, has been heavily studied as a biomarker for TB, but with little success due to its complexation with endogenous components of body fluids in a manner that sterically interferes with its detection by ELISA and other immunoassays. Recent work by our group and others has shown that complexation can be disrupted with protein-denaturing protocols. By way of followup, we recently described an enzymatic digestion (Proteinase K) sample pretreatment that enables quantitative recovery of ManLAM spiked into healthy human control serum. Herein, we report on the transfer of our benchtop sample pretreatment methodology to an automated microfluidic platform. We show that this platform can be configured to: (1) carry out the pretreatment process with very little user interaction and, (2) yield recoveries for ManLAm spiked into control serum which are statistically indistinguishable from those achieved by the benchtop process. Plans to integrate this device with a portable sample reader as a possible basis for a PoC TB diagnostic system and analyze patient samples are briefly discussed.

Introduction

The development of a point-of-care (PoC) diagnostic test for tuberculosis (TB) continues to be a high priority in global healthcare.[1–3] According to the latest estimates from the World Health Organization, there were 7.5M people newly infected with TB in 2022 and 1.3M TB-associated deaths.[4] The vast majority of this continuing mortality occurs in low- and middle-income countries (LMICs), which largely reflects the absence of clinically accurate and affordable PoC tests for TB. The need for such capabilities is underscored by the fact that TB is curable if detected early in its progression, but suffers a case fatality rate of ~50% if left untreated.[5]

We recently reported on the development of an approach to the detection of mannose-capped lipoarabinomannan (ManLAM), a TB biomarker of growing importance.[6–9] ManLAM, a highly-branched lipoglycan (~17.3 kDa[10]), constitutes ~15% of the total mass of the *Mycobacterium tuberculosis* (Mtb) bacillus.[11] It is an important virulence factor in the infectious pathology of Mtb and is actively and passively shed into the circulatory system of an infected individual.[12–14] It is not surprising that, given these characteristics, there has been a great deal of interest in assessing the potential merits of ManLAM as an accurate antigenic marker for TB.[1] Examples of these efforts include the use of enzyme-linked immunosorbent assays (ELISA) and other immunoassay architectures to measure ManLAM in urine, serum, and other body fluids.[6–8,15–24]

Most of the early work on ManLAM, however, suffered from unacceptably poor levels of clinical accuracy, especially when targeted at early-stage infection.[15,17,21,24] Recent insights from a team at Los Alamos National Laboratory,[22,23] our work with Colorado State University,[6–8,18–20] and others[16,25,26] have begun to change this picture. These efforts have shown that: (1) ManLAM is present in serum and urine in not only its free form, but also in one or more complexed forms; (2) complexation sterically interferes with the capture and/or labeling of ManLAM in an immunoassay; (3) complexation can be countered by means of a protein-denaturing protocol

[e.g., acidification with perchloric acid[6,7] or enzymatic digestion with Proteinase K (ProK)[9,18,27]]; and (4) breaking up the complex improves the detectability of ManLAM by as much as 250×, depending on the method of readout.[7,9] These findings have rekindled interest in the use of ManLAM as a biomarker of TB.[1]

Along these lines, we recently reported on an investigation aimed at maximizing the recovery of ManLAM from human serum by fine-tuning the conditions used for ProK digestion.[9] When accounting for a small, quantitatively reproducible level of sample concentration, the optimal enzymatic digestion conditions identified in that work yielded a recovery factor of 98% ± 13% for samples prepared by spiking ManLAM into control human serum. The work described herein translates this method to a prototype microfluidic system that has the potential to facilitate the movement of sample pretreatment from a laboratory benchtop process to PoC applications.[4,28] This paper details the design and operation of a functional prototype capable of obtaining ManLAM recoveries indistinguishable from those obtained using the benchtop process and demonstrates the potential for automating the sampled preparation process. Plans to further refine the technology and apply it to the analysis of TB patient samples are briefly discussed.

Experimental Details

ManLAM samples and pretreatment

Preparation

Samples were prepared by spiking culture-harvested ManLAM into healthy control human serum. Sufficient volumes (1.5 mL) of each sample were prepared so that one portion could be applied to assess the effectivensss of microfluidic processing with respect to ManLAM recovery, and another portion could be used to run benchtop-processed controls per our previously-

reported protocol.[9] All samples were left to stand overnight at 4 °C to allow complete complexation of ManLAM with the sample matrix.

Benchtop serum pretreatment

The protocol used for the benchtop pretreatment has been previously described.[9,18] Briefly, 500 µL serum samples were: (1) spiked with 5 µL ProK from an as-received stock solution (20 mg/mL), reaching a final concentration of 200 µg/mL, (2) mixed by vortexing, and (3) immediately placed in a dry bath (Fisher Isotemp) at 55 °C for 30 min. The samples were then transferred to a boiling water bath and incubated for ten min, which served to deactivate ProK and precipitate digested proteins. Next, samples were centrifuged at 12,000 × g for five min to pellet the precipitate. Finally, the supernatant was carefully separated from the pellet for analysis by ELISA. All benchtop samples were processed in parallel.

Microfluidic serum pretreatment

The protocol used for microfluidic pretreatment adhered as closely as possible to the benchtop protocol, with only two minor deviations. First, due to the constraints of the microfluidic platform, the minimum volume that we could comfortably handle was 20 µL for the reagent metering chamber. Thus, it was necessary to dilute the ProK stock solution so that this larger volume could be used while maintaining the same final ProK concentration. We diluted the as-received ProK stock solution 1:4 in 50 mM tris buffer (pH 8). Second, rather than vortexing, the sample and dilute ProK solution were mixed by shuttling the combined liquids back-and-forth between the two sample chambers (see **Fig. 2** and associated discussion). Samples pretreated using the microfluidic platform were processed in a random sequence, which allowed for examination of ManLAM carryover.

ManLAM quantitation

ManLAM was measured using our previously-described ELISA.[8] This sandwich ELISA uses a polyclonal rabbit antibody for antigen capture and a monoclonal human antibody to label the captured antigen, and consistently reaches a limit of detection of ~10 pg/mL. The details of the ELISA are reproduced in the Supplementary Information.

Materials and reagents

A bill of materials used to construct the prototype microfluidic device is included in the Supplementary Information. Proteinase K [recombinant, PCR grade, 10 mM Tris-HCl (pH 7.5), containing calcium acetate and 50 % (v/v) glycerol] was from Thermo Scientific. ManLAM from Mtb strain CDC 1551 was kindly provided by Dr. Delphi Chatterjee at Colorado State University. Pooled human serum, type AB, was from Innovative Research, Inc. (catalog # ISERAB). Tris(hydroxymethyl)aminomethane and hydrochloric acid (used to prepare the pH 8 tris buffer for ProK dilution) were from Fisher Scientific and Sigma-Aldrich, respectively. All aqueous solutions were prepared in ultrapure water (18.2 MΩ cm resistivity), which was purified by passage through a house deionization plant and a Barnstead Nanopure system. The materials and reagents used to perform the ELISA are listed in the Supplementary Information.

Design

Figure 1 presents a schematic outlining the critical functions to be performed by the microfluidic sample pretreatment platform. We chose to construct an externally controlled pneumatic microfluidic device (ECPMD), a style of microfluidic device which has been shown to be readily adapted to a wide range of fluid mixing and metering processes.[29–34] Our ECPMD consists of three main components: (1) a fluid-handling layer that contains the fluid channels; (2) a control layer that consists of cavities for valves and chambers connected by tubing to the

external pneumatic system and controller; and (3) a flexible membrane that separates the fluid-handling layer from the control layer and deforms in response to applied pneumatic inputs, opening and closing each of the valves and chambers in the fluid-handling layer (**Figure S-1**).

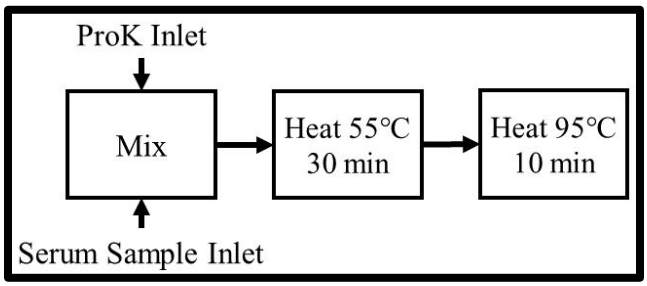

Figure 1. Operational schematic showing the process flow for the microfluidic ManLAM pretreatment platform.

ECPMDs are commonly manufactured using poly(dimethylsiloxane) (PDMS) for all three layers, with microheaters mounted on underlying glass slides for temperature manipulation.[35–38] These microheaters are, however, ineffective in heating large sample volumes, such as the 500 µL samples used in our platform. We first attempted to overcome this obstacle by fully immersing an entirely PDMS platform in a heated water bath. However, due to the low thermal conductivity of PDMS (0.2 W m^{-1} K^{-1} [39]), the time required to reach a temperature of 95 °C was unreasonably long. As a solution, we switched to a control layer made from aluminum, which has a much higher thermal conductivity (167 W m^{-1} K^{-1} [40]). We also switched to a ceramic cartridge heater that, when inserted into the aluminum control layer, proved to be much more effective in rapidly reaching the desired temperatures for enzymatic digestion and enzyme deactivation.

Figure 2A presents the layout of the microfluidic platform. The reagent and sample inlets are the entry points for the ProK solution and sample, respectively, which were supplied from a pipette tip reservoir mounted in each inlet via. The reagent inlet opens into a 20 µL metering chamber (Chamber 1), while the sample inlet opens directly into a sample metering and mixing chamber (Chamber 2). Chambers 2 and 3, each 500 µL, are used for metering the sample and

mixing the sample with the ProK solution. These two chambers are controlled independently; the sample is shuttled back-and-forth between chambers for mixing by cycling the chambers between alternating open/closed states. After completing the digestion and deactivation steps the sample is sent to the outlet port, where it is collected in a pipette tip reservoir for transfer to a microcentrifuge tube. The inlets and outlet are isolated by Quake-type valves to control downstream fluid flow; Chamber 1 is likewise isolated from Chamber 2.[41] The operation of the microfluidic platform is discussed in detail below.

Fabrication

Fluid-handling layer

The fluid-handling layer was fabricated using soft lithography.[42] PDMS casts were made from single-sided acrylic and polystyrene molds. A double-sided silicone adhesive (silicone adhesive 1) was applied to a 1 mm PMMA sheet and the adhesive, backing, and PMMA were cut using a CO_2 laser (Universal Laser Systems VLS 3.60, 100 W). The second backing was removed from the adhesive and the PMMA was adhered to the bottom of a polystyrene petri dish to form a mold. PDMS was added to the mold and cured at 70 °C for 3 h. The PDMS castings were then removed from the molds, the perimeter was trimmed to size, and vias were cored with a 1.5 mm biopsy punch for inlets and outlets. An acrylic pressure plate was laser cut and used to secure the PDMS layer, making a tight seal to the control layer below.

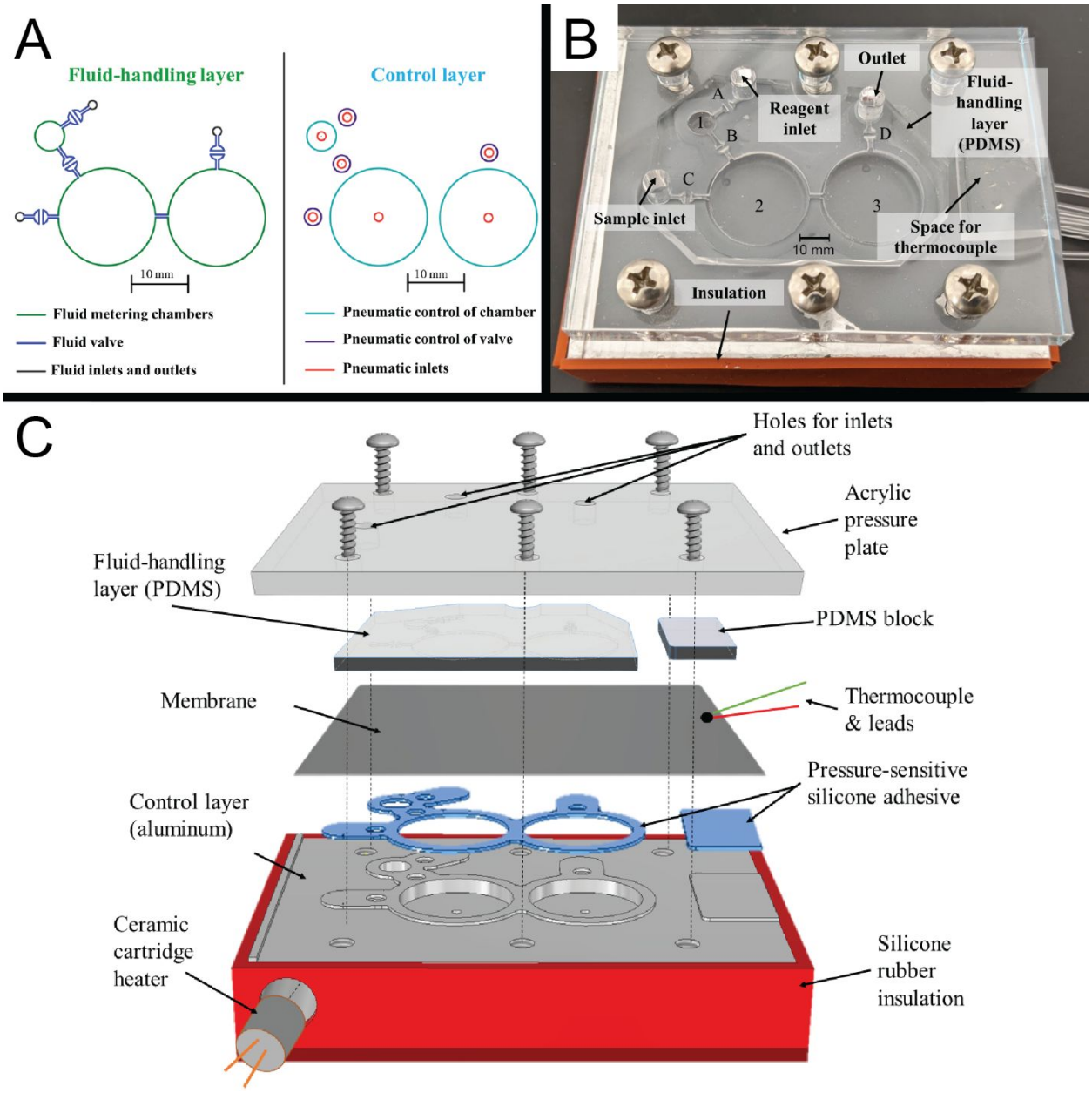

Figure 2. (A) Schematic of the fluid and control layers for the prototype device. (B) Photograph of the assembled device. Valves are labeled from A – D and chambers are labeled from 1 – 3. Valves are shown in a closed state while chambers remain in an open state. The external pneumatic control system is not pictured. (C) Schematic view of the platform as assembled.

Control layer

The control layer was manufactured by machining an aluminum block using a tabletop mill (Model 3040T, Automation Technology, Inc.). To improve temperature stability, the aluminum block was insulated using silicone rubber (**Figs. 2B** and **C**). Recessed cylindrical spaces

surrounded by elevated rings (0.5 mm in height, similar to a tongue face flange) were cut for each valve and chamber. The elevated ring ensured that the silicone membrane formed a tight seal to the control layer. The aluminum block was drilled and tapped for the bolts used to hold the pressure plate in place, and a hole was drilled for the ceramic cartridge heater, sized so that the heater was held in place with a friction fit.

Assembly

Figure 2B shows a photograph of the assembled chip, and **Figure 2C** illustrates how the components fit together. Silicone adhesive 2 was laser cut and bonded to the elevated gasket seal on the aluminum housing. A silicone membrane was bonded to the silicone adhesive via air plasma bonding[43,44] to create a sealed and isolated compartment for each chamber and valve. The PDMS fluid-handling layer was carefully aligned with the aluminum control layer; to aid alignment, vacuum was applied to all valves and chambers, deforming the silicone membrane to clearly show their positions. A thermocouple was placed adjacent to the mixing chambers and a small piece of PDMS was placed atop it to secure it in place. The acrylic pressure plate was set in place and the six bolts were carefully tightened in a uniform and alternating pattern to ensure a leak-tight seal.

A ceramic cartridge heater was inserted into a small-diameter hole bored into the side of the control layer and connected to a power supply and PID controller. The PID controller utilized the aforementioned thermocouple for temperature control. Individual pneumatic control lines were potted in each cavity of the control layer using two-part epoxy. This setup operated consistently without leaking or failure over several hundred valve cycles at temperatures ranging from 25°C to 100°C and pressures up to 30 psi.

Pneumatic control system

The pneumatic control lines were operated by a custom-built array of three-way pneumatic micro-valves capable of delivering three different pressures or vacuum levels. The microfluidic platform was connected to the pneumatic valves using standard 1/16 in. barb fittings and 1/16 in. Tygon tubing. The valve array was controlled using a custom script written in Python. A pressure of 7 psi was used to close the chambers while 12 psi was used to close the valves; both chambers and valves were opened by the application of a low vacuum from a house line.

Operation

The initial condition of the pneumatic control system was programmed to set all chambers and valves to a closed state and the aluminum control layer was at room temperature. The sample and ProK solution were loaded into pipette tips connected to the sample and reagent inlet ports, respectively. Valve A and Chamber 1 were opened, filling Chamber 1 with ProK solution. Once Chamber 1 had filled, Valve A was closed to prevent backflow into the reagent reservoir. Valve C was opened, followed by Chamber 2, filling Chamber 2 with 500 µL of sample. Valve C was closed, Valve B was opened, and Chamber 1 was closed, pushing the ProK solution into Chamber 2. The PDMS flexes in response to applied pressure from Chamber 1 and the 520 µL volume is easily accommodated. Valve B was then closed to prevent backflow into Chamber 1.

To mix the sample, Chambers 2 and 3 were simultaneously switched between opposite states (i.e., 2 closed, 3 open to 2 open, 3 closed) to shuttle the sample back-and-forth between the two chambers. This process was repeated ten times, taking no more than ten seconds in total. The platform was then heated to 55 °C for 30 min, while the ProK digested the proteins in the sample matrix. Next, the platform was heated to for ten min, which deactivated the enzyme and caused the precipitation of digestion products.[9] Finally, the processed sample was transferred to the

outlet reservoir by opening Valve D and closing Chamber 2 and then Chamber 3. The system was reset by returning the heater to room temperature and flushing the platform with 40 mL of ultrapure water using an automated sequence that washed all of the valves and chambers on the platform.

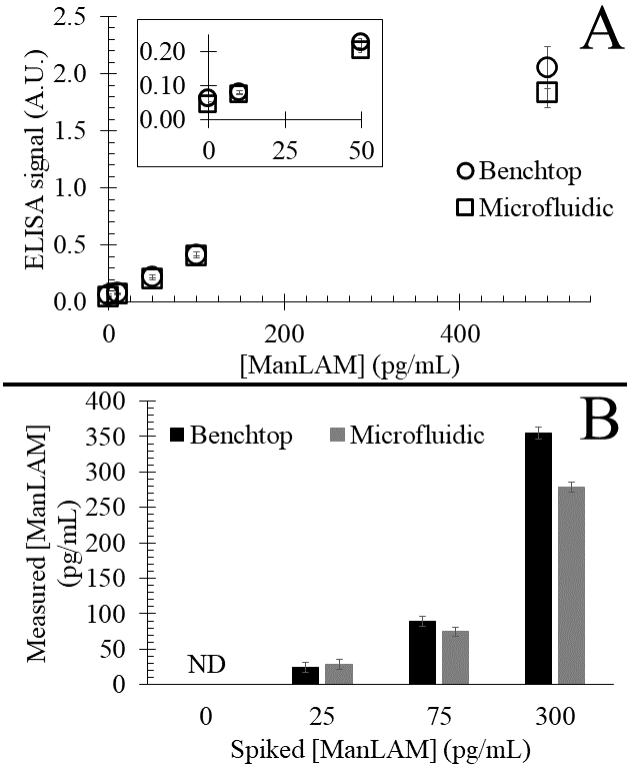

Figure 3. (A) Samples over a range of ManLAM concentrations from 10 to 500 pg/mL were processed on the microfluidic platform and the bench and the ELISA responses were measured. Inset: Enlarged view of the low-concentration regime. Error bars represent the standard deviation of three replicate measurements. (B) A set of samples were prepared with the microfluidic and benchtop operators blinded to their ManLAM concentrations, processed, and analyzed against ManLAM standards prepared in an innocuous buffered matrix (**Figure S-2**) to determine the ManLAM concentration. Error bars represent the standard deviation of three replicate measurements.

Performance Comparison

To compare the microfluidic digestion to the benchtop digestion, a series of serum samples spiked with ManLAM (10 – 500 pg/mL) were prepared and processed by both procedures. As shown in **Figure 3A**, the measured ELISA responses for the two sets of experiments are nearly identical; no significant difference was observed at the 95% confidence interval by a student's t-test (see **Table S-1**).[45] The limit of detection, measured as the average signal from the blank plus

three times its standard deviation,[46,47] was slightly lower for the samples processed on the microfluidic platform (4 pg/mL) than for those processed by the benchtop protocol (13 pg/mL), owing to a slightly lower blank signal for that set of samples.

To apply the microfluidic platform to a more realistic scenario of determining an unknown ManLAM concentration in a sample, a set of samples were prepared by a third party with the microfluidic and benchtop operators blinded to their actual concentrations. The samples were processed and their ManLAM concentrations determined by comparison to a standard curve prepared in an innocuous buffered matrix (**Figure S-2**). As in our previously reported work,[9] the measured concentrations were corrected for the preconcentration effect (16% concentration increase) that results from a decrease in supernatant volume relative to the initial sample volume during sample pretreatment. The sample concentrations were then unblinded for comparison. **Figure 3B** shows the results of this experiment. There is no significant difference between pretreatment methods with 95% confidence (**Table S-2**). All samples were correctly identified as positive or negative for ManLAM, with the blank sample coming in below the limit of detection of the calibration curve prepared in MPBS+BSA (7 pg/mL) and the measured concentrations accurate to within 20% of the spiked concentrations.

Most of the samples processed on the chip showed a slightly lower concentration than those processed on the bench, with an average difference of –6%. We attribute the slightly reduced recovery on chip to the loss of ManLAM due to its adsorption on the walls of the microfluidic system. Future work will include an investigation of other materials from which the fluid-handling layer can be constructed in an attempt to combat ManLAM adsorption.

The blinded experiment also demonstrated that it was possible to wash and reuse a single microfluidic chip between samples with no detectable carryover of ManLAM. The highest-

concentration sample was run immediately prior to the blank, yet the blank exhibits no evidence of contamination. We note that this does not preclude the aforementioned possibility of adsorption of ManLAM to the chip materials, as strongly adsorbed ManLAM may not release to cause carryover or the rinsing protocol may completely remove any adsorbed ManLAM before the next sample is processed.

Discussion and Conclusion

Our findings indicate that the multilayer ECPMD chip can be used as an effective and partially automated alternative to the manual benchtop process. The software enables automatic reagent and sample metering, mixing, incubation, and temperature control on the chip. In this way, a user needs only to supply the sample, initiate the automated protocol for ProK digestion, and collect the processed sample. The performance of this device as measured by the recovery of ManLAM spiked into healthy control human serum samples was statistically indistinguishable from that of the original benchtop protocol. This represents an important proof of concept, demonstrating that sample pretreatment for ManLAM analysis can be automated for operation by the non-specialist user.

While this platform was designed for TB diagnostics, it could also be readily adapted to a number of other diagnostic sample preparation protocols that require liquid metering, mixing, and temperature control. Metering is performed by the fixed volume of the cavities in the control layer. The range of volumes possible is quite large, ranging from microliters to milliliters, which can allow this system to integrate with a wide variety of diagnostic tests, including analysis of body fluids (e.g., analysis of serum for galactomannan as a biomarker of invasive aspergillosis[48] or *Histoplasma* antigen as a biomarker of histoplasmosis[49]) and environmental samples (e.g., wastewater). Most microfluidic passive mixing methods are incapable of mixing viscous fluids

due to difficulties in establishing turbulence.[50] In our case, mixing is achieved by shuttling the fluid between two chambers connected by a short channel, with passage of the sample through the channel giving rise to turbulent (active) mixing regardless of fluid viscosity.

Composite microfluidic systems comprised of PDMS and milled materials are of considerable value as combining the properties of the various materials (e.g., thermal resistance, elasticity, hardness) enables unique capabilities. This work demonstrates the combination of milled aluminum, silicone, and laser-cut acrylic to achieve an elevated temperature (up to 100 ° C) and pressure stable (30 psi) system that was required by the assay.

Our next steps will include coupling this device to microfluidic filtration and ManLAM detection systems, with the latter based on our previously-developed immunoassays for ManLAM.[6–9] Some minor refinements to this device are also possible, including the addition of multiple temperature zones, so that the sample can transition from the digestion temperature to the deactivation temperature without waiting for the temperature of the chip to rise. This could be achieved by incorporating isolated aluminum heating blocks into a control layer otherwise composed of a thermally-insulating material such as PDMS, poly(lactic acid) (PLA), or acrylonitrile butadiene styrene (ABS) (with the latter two capable of being fabricated via fused deposition modeling 3D printing). Additionally, a multiplex device could be created to simultaneously process multiple samples. Plans are also being developed to carry out an initial clinical trial utilizing biobanked patient samples to demonstrate the efficacy of ManLAM detection in ProK-pretreated serum for rapid, sensitive, and accurate diagnosis of TB.

Author Contributions

Christopher J. Lambert: Investigation, Methodology, Software, Visualization, Writing – Original Draft Preparation. **Eamonn Clarke**: Formal Analysis, Investigation, Methodology,

Visualization, Writing – Review & Editing. **Dhruv Patel**: Investigation, Software, Visualization, Writing – Review & Editing. **Lars B. Laurentius**: Investigation, Resources, Validation. **Bruce K. Gale**: Supervistion. **Himanshu J. Sant**: Conceptualization, Funding Acquisition, Project Administration, Supervision, Writing – Original Draft Preparation. **Marc D. Porter** – Conceptualization, Funding Acquisition, Project Administration, Supervision, Writing – Review & Editing.

Conflicts of Interest

There are no conflicts of interest to declare.

Acknowledgements

The authors gratefully acknowledge the support of this work from SBIR I contract 75N93019C00023 "Mobile Health Point-of-Care Diagnostics for Tuberculosis." EC gratefully acknowledges the support of a Graduate Research Fellowship from the Immunology, Inflammation, and Infectious Disease (3i) Initiative at the University of Utah. We also acknowledge the assistance of Brady Goenner in developing the Python code used to run the microfluidic platform.

References

1 J. Flores, J. C. Cancino and L. Chavez-Galan, *Front. Microbiol.*, 2021, **12**, 638047.
2 S. Gupta and V. Kakkar, *Biosens. Bioelectron.*, 2018, **115**, 14–29.
3 K. Dheda, M. Ruhwald, G. Theron, J. Peter and W. C. Yam, *Respirology*, 2013, **18**, 217–232.
4 World Health Organization, *Global tuberculosis report 2023*, Geneva, 2023.
5 E. W. Tiemersma, M. J. van der Werf, M. W. Borgdorff, B. G. Williams and N. J. D. Nagelkerke, *PLoS One*, 2011, **6**, e17601.
6 L. B. Laurentius, A. C. Crawford, T. S. Mulvihill, J. H. Granger, R. Robinson, J. S. Spencer, D. Chatterjee, K. E. Hanson and M. D. Porter, *Analyst*, 2017, **142**, 177–185.
7 A. C. Crawford, L. B. Laurentius, T. S. Mulvihill, J. H. Granger, J. S. Spencer, D. Chatterjee, K. E. Hanson and M. D. Porter, *Analyst*, 2017, **142**, 186–196.
8 N. A. Owens, C. C. Young, L. B. Laurentius, P. De, D. Chatterjee and M. D. Porter, *Anal.*

Chim. Acta, 2019, **1046**, 140–147.
9 E. Clarke, R. Robinson, L. B. Laurentius and M. D. Porter, *Anal. Chem.*, 2023, **95**, 9191–9198.
10 A. Venisse, J. M. Berjeaud, P. Chaurand, M. Gilleron and G. Puzo, *J. Biol. Chem.*, 1993, **268**, 12401–12411.
11 S. W. Hunter, H. Gaylord and P. J. Brennan, *J. Biol. Chem.*, 1986, **261**, 12345–12351.
12 S. D. Lawn, *BMC Infect. Dis.*, 2012, **12**, 103.
13 L. M. Pereira Arias-Bouda, L. N. Nguyen, L. M. Ho, S. Kuijper, H. M. Jansen and A. H. J. Kolk, *J. Clin. Microbiol.*, 2000, **38**, 2278–2283.
14 B. Al-Sayyed, S. Piperdi, X. Yuan, A. Li, G. S. Besra, W. R. Jacobs, A. Casadevall and A. Glatman-Freedman, *Tuberculosis*, 2007, **87**, 489–497.
15 S. D. Lawn, D. J. Edwards, K. Kranzer, M. Vogt, L.-G. Bekker and R. Wood, *AIDS*, 2009, **23**, 1875–1880.
16 C. E. Chan, S. Götze, G. T. Seah, P. H. Seeberger, N. Tukvadze, M. R. Wenk, B. J. Hanson and P. A. MacAry, *Sci. Rep.*, 2015, **5**, 10281.
17 R. Wood and S. D. Lawn, *Expert Rev. Mol. Diagn.*, 2012, **12**, 549–551.
18 A. G. Amin, P. De, J. S. Spencer, P. J. Brennan, J. Daum, B. G. Andre, M. Joe, Y. Bai, L. Laurentius, M. D. Porter, W. J. Honnen, A. Choudhary, T. L. Lowary, A. Pinter and D. Chatterjee, *Tuberculosis*, 2018, **111**, 178–187.
19 N. A. Owens, L. B. Laurentius, M. D. Porter, Q. Li, S. Wang and D. Chatterjee, *Appl. Spectrosc.*, 2018, **72**, 1104–1115.
20 N. A. Owens, A. Pinter and M. D. Porter, *J. Raman Spectrosc.*, 2019, **50**, 15–25.
21 K. Reither, E. Saathoff, J. Jung, L. T. Minja, I. Kroidl, E. Saad, J. F. Huggett, E. N. Ntinginya, L. Maganga, L. Maboko and M. Hoelscher, *BMC Infect. Dis.*, 2009, **9**, 141–151.
22 H. Mukundan, S. Kumar, D. N. Price, S. M. Ray, Y. J. Lee, S. Min, S. Eum, J. Kubicek-Sutherland, J. M. Resnick, W. K. Grace, A. S. Anderson, S. H. Hwang, S. N. Cho, L. E. Via, C. Barry, R. Sakamuri and B. I. Swanson, *Tuberculosis*, 2012, **92**, 407–416.
23 R. M. Sakamuri, D. N. Price, M. Lee, S. N. Cho, C. E. Barry, L. E. Via, B. I. Swanson and H. Mukundan, *Tuberculosis*, 2013, **93**, 301–307.
24 J. Minion, E. Leung, E. Talbot, K. Dheda, M. Pai and D. Menzies, *Eur. Respir. J.*, 2011, **38**, 1398–1405.
25 T. Broger, M. P. Nicol, G. B. Sigal, E. Gotuzzo, A. J. Zimmer, S. Surtie, T. Caceres-Nakiche, A. Mantsoki, E. I. Reipold, R. Székely, M. Tsionsky, J. van Heerden, T. Plisova, K. Chikamatsu, T. L. Lowary, A. Pinter, S. Mitarai, E. Moreau, S. G. Schumacher and C. M. Denkinger, *J. Clin. Invest.*, 2020, **130**, 5756–5764.
26 A. G. Amin, P. De, B. Graham, R. I. Calderon, M. F. Franke and D. Chatterjee, *Sci. Rep.*, 2021, **11**, 1–13.
27 Y. Panraksa, A. G. Amin, B. Graham, C. S. Henry and D. Chatterjee, *PLoS One*, 2021, **16**, 1–15.
28 S. V. Kik, in *High-priority target product profiles for new tuberculosis diagnostics: report of a consensus meeting*, World Health Organization, Geneva, 2014, pp. 11–18.
29 X. Zhou, X. Zhou and B. Zheng, *Biomicrofluidics*, 2013, **7**, 054116.
30 C.-F. Lin, G.-B. Lee, C.-H. Wang, H.-H. Lee, W.-Y. Liao and T.-C. Chou, *Biosens. Bioelectron.*, 2006, **21**, 1468–1475.
31 S. Mangru, B. L. Bentz, T. J. Davis, N. Desai, P. J. Stabile, J. J. Schmidt, C. B. Millard, S.

Bavari and K. Kodukula, *SLAS Discov.*, 2005, **10**, 788–794.
32 S.-W. Nam, D. Van Noort, Y. Yang and S. Park, *Lab Chip*, 2007, **7**, 638.
33 W. H. Grover, R. H. C. Ivester, E. C. Jensen and R. A. Mathies, *Lab Chip*, 2006, **6**, 623.
34 M. Hitzbleck and E. Delamarche, *Chem. Soc. Rev.*, 2013, **42**, 8494.
35 B. T. Chia, H.-H. Liao and Y.-J. Yang, *Sensors Actuators A Phys.*, 2011, **165**, 86–93.
36 F. Yu, R. Deng, W. Hao Tong, L. Huan, N. Chan Way, A. IslamBadhan, C. Iliescu and H. Yu, *Sci. Rep.*, 2017, **7**, 14528.
37 P. S. Chee, M. N. Minjal, P. L. Leow and M. S. M. Ali, *Sensors Actuators A Phys.*, 2015, **233**, 1–8.
38 B. T. Chia, H.-H. Liao and Y.-J. Yang, in *TRANSDUCERS 2009 - 2009 International Solid-State Sensors, Actuators and Microsystems Conference*, IEEE, 2009, pp. 2286–2289.
39 S. Vlassov, S. Oras, M. Timusk, V. Zadin, T. Tiirats, I. M. Sosnin, R. Lõhmus, A. Linarts, A. Kyritsakis and L. M. Dorogin, *Materials (Basel).*, 2022, **15**, 1652.
40 MatWeb, Aluminum 6061-T6; 6061-T651, https://asm.matweb.com/search/SpecificMaterial.asp?bassnum=ma6061t6, (accessed 19 April 2024).
41 M. A. Unger, H.-P. Chou, T. Thorsen, A. Scherer and S. R. Quake, *Science*, 2000, **288**, 113–116.
42 J. C. Mcdonald, D. C. Duffy, J. R. Anderson and D. T. Chiu, *Electrophoresis*, 2000, **21**, 27–40.
43 M. A. Eddings, M. A. Johnson and B. K. Gale, *J. Micromechanics Microengineering*, 2008, **18**, 067001.
44 A. Borók, K. Laboda and A. Bonyár, *Biosensors*, 2021, **11**, 292.
45 D. C. Harris and C. A. Lucy, in *Quantitative Chemical Analysis*, W. H. Freeman, New York, NY, Ninth Edit., 2016, pp. 74–79.
46 D. C. Harris and C. A. Lucy, in *Quantitative Chemical Analysis*, W. H. Freeman, New York, NY, Ninth Ed., 2016, pp. 102–103.
47 D. A. Skoog, F. J. Holler and S. R. Crouch, in *Principles of Instrumental Analysis*, Brooks/Cole, Belmont, CA, Sixth Ed., 2007, p. 20.
48 L. J. Wheat, *Transpl. Infect. Dis.*, 2003, **5**, 158–166.
49 S. Swartzentruber, A. LeMonte, J. Witt, D. Fuller, T. Davis, C. Hage, P. Connolly, M. Durkin and L. J. Wheat, *Clin. Vaccine Immunol.*, 2009, **16**, 320–322.
50 K. Ward and Z. H. Fan, *J. Micromechanics Microengineering*, 2015, **25**, 094001.

Microfluidic Platform for the Enzymatic Pretreatment of Human Serum for the Detection of the Tuberculosis Biomarker Mannose-Capped Lipoarabinomannan

Christopher J. Lambert[1]*, Eamonn Clarke[2†], Dhruv Patel[1†], Lars B. Laurentius[3], Bruce K. Gale[1], Himanshu J. Sant[1†], Marc D. Porter[2,4‡]
Departments of Mechanical Engineering[1], Chemistry[2], Electrical and Computer Engineering[3] and Chemical Engineering[4], University of Utah, Salt Lake City, UT, USA 84112
*Present address: Colossal Biosciences, Austin, TX, USA 78701
[†]Present address: Department of Chemical Engineering, University of Utah, Salt Lake City, UT, USA 84112
[‡]Author to whom correspondence should be addressed

Data availability statement

The data supporting this article are provided in the main text and Supplementary Information. Additional information is available from the corresponding author on request.